

Flying spin qubits: A method for encoding and transporting qubits within a dimerized Heisenberg spin- $\frac{1}{2}$ chain

Vanita Srinivasa* and Jeremy Levy†

Department of Physics and Astronomy, University of Pittsburgh, Pittsburgh, Pennsylvania 15260, USA

C. Stephen Hellberg‡

Code 6390, Center for Computational Materials Science, Naval Research Laboratory, Washington, DC 20375, USA

(Received 4 May 2007; published 21 September 2007)

We present a method for encoding and transporting qubits within a dimerized Heisenberg spin- $\frac{1}{2}$ chain. Logical qubits are localized at the domain walls that separate the two possible dimerized states. The domain walls can be moved to produce “flying spin qubits.” The topological nature of these states makes them stable against local perturbations of the exchange profile. Pairs of domain walls can be used to generate Einstein-Podolsky-Rosen pairs of entangled qubits. We discuss speed limitations within an exactly solvable three-spin model and describe a possible physical realization using quantum dot arrays.

DOI: [10.1103/PhysRevB.76.094411](https://doi.org/10.1103/PhysRevB.76.094411)

PACS number(s): 75.10.Pq, 75.10.Jm, 03.67.Lx, 73.21.La

I. INTRODUCTION

Spin angular momentum forms the basis for quantum bits (qubits) in several quantum computing architectures.^{1–7} In many proposals, logical quantum bits are formed from the 2^m -dimensional Hilbert space corresponding to m spins.^{8–11} Such encoding schemes are useful for implementing quantum error correction¹² as well as for matching specific material systems to experimental capabilities. For example, by using two or more spins, one can define logical qubits for which universal quantum gating is achieved using only the Heisenberg exchange interaction.^{10,11} Exchange-coupled spin clusters also form energetically stable qubits by virtue of the ground state doublet that is characteristic of the energy level spectrum for these systems.¹³ The Jordan-Wigner spin-particle mapping in one¹⁴ or more^{15,16} dimensions suggests a wide range of candidate qubits one might construct from interacting spins.

The need for “flying qubits,”¹⁷ i.e., a mechanism for rapidly transporting quantum information, has long been recognized as a weakness of spin-based quantum computing architectures. Several different methods have been proposed to implement long-range transport of quantum information. One method involves coupling spin qubits to an external “quantum bus,” e.g., an optical cavity mode.⁴ Such an approach typically introduces an entirely new set of constraints, and engineering strong optical couplings can be challenging in practice. Another approach attempts quantum information transfer along exchange-coupled spin chains.^{18–21} While theoretically possible, the fidelity of transmission depends critically on the values of the coupling strengths between the spins in the chain, making this approach susceptible to errors. Additionally, the use of multiple swap operations between nearest-neighbor single spins is not optimal for long-range transport in one-dimensional spin chains because of the large number of precise gate operations required and the relatively low error threshold for quantum error correction.^{22,23} Finally, the quantum teleportation protocol²⁴ of Bennett *et al.* employs the generation and transport of Einstein-Podolsky-Rosen (EPR) pairs to teleport qubits to their needed location.

Here, we present a qualitatively different approach to the construction of flying qubits. The method relies on the design of a spin-based “designer quantum field,” constructed from a one-dimensional dimerized Heisenberg spin- $\frac{1}{2}$ chain. Logical qubits are localized at the domain walls that separate the two possible dimerized states. Unlike previous encoding schemes,^{8–11} logical qubits are not associated with a definite number of spins; rather, these “defect” states exist even when the number of spins approaches infinity. Their topological nature²⁵ makes them stable with respect to local perturbations of the exchange profile. By moving the domain walls, it is possible to produce “flying spin qubits.” Below, we explore the properties of this class of systems both analytically for small chains (three spins) and numerically for larger chains (up to 30 spins). Numerical studies for the larger chains are carried out using the Lanczos method of diagonalization.²⁶

II. DIMERIZED SPIN CHAINS

A one-dimensional system of spin- $\frac{1}{2}$ objects interacting via nearest-neighbor Heisenberg exchange is described by the following effective Hamiltonian:

$$H = \sum_{k=1}^{n_c} J_k (\mathbf{S}_k \cdot \mathbf{S}_{k+1}) \equiv \sum J_k (\mathbf{S}_k \cdot \mathbf{S}_{k+1}), \quad (1)$$

where $S_k = (X_k, Y_k, Z_k)$ are Pauli operators for the k th spin, $\{J_k > 0\}$ quantify the strength of nearest-neighbor exchange interactions, and periodic boundary conditions apply if $k \pm n_c \equiv k$. In the absence of external magnetic fields, the total spin angular momentum operator $S^2 = (\sum \mathbf{S}_k)^2$ as well as the total z component $S_z = \sum Z_k$ commute with H , so one may work within subspaces of definite S_z and/or S^2 .

To illustrate the properties of the dimerized Heisenberg spin systems investigated here, we initially consider an open, symmetric chain having an odd number of spins n_c and a single kink in the center [Fig. 1(a)]. The dimerization of the chain is described by a parameter a , such that $\{J_{2d} = J_{n_c - 2d}$

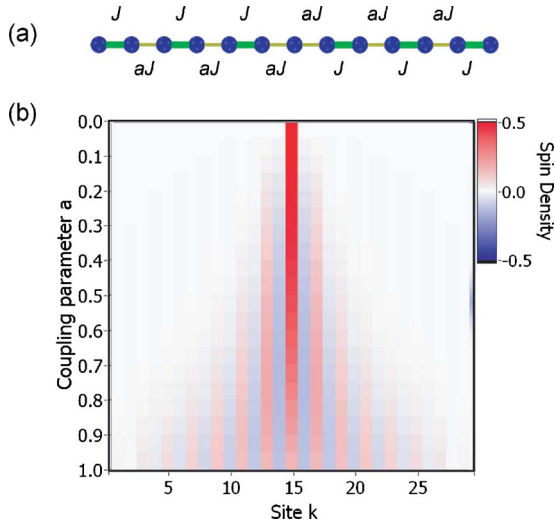


FIG. 1. (Color online) Dimerized Heisenberg spin- $\frac{1}{2}$ chains. (a) Schematic of an open Heisenberg-coupled spin chain ($n_c=13$) with a single defect at the center. (b) Plot of spin density for the $S_Z=1/2$ ground state as a function of the dimer coupling parameter a for the case $n_c=29$.

$=aJ; J_{2d-1}=J_{n_c-2d+1}=J, d=1, 2, \dots, (n_c-1)/4\}$ and $0 \leq a \leq 1$. Because the system contains an odd number of spins, the minimum total spin angular momentum (corresponding to the ground state) is $S=1/2$ ($\hbar=1$); here, we consider the $S_Z=1/2$ “spin-up” subspace, but an identical analysis applies for the $S_Z=-1/2$ “spin-down” subspace. The ground state is calculated by numerical diagonalization of the Hamiltonian in Eq. (1) as a function of a , and the spin density $\langle Z_k \rangle$ can be computed [Fig. 1(b)]. The case $a=0$ corresponds to a single spin localized at the center of the chain, surrounded by uncoupled dimers on either side. The spin chain may be initialized in this configuration by cooling the system to the ground state. As a is increased, the spin density becomes more delocalized. The uniform open spin chain ($a=1$) has already been investigated within the context of quantum computation and forms a well-defined “spin cluster qubit.”¹³ Adiabatic variation of a between 0 and 1 provides an explicit mechanism for interconversion between a single isolated spin and a delocalized spin cluster state, allowing an initially stationary qubit to be transformed into a movable flying spin qubit. After transporting the qubit to another location, the transformation may be reversed to reproduce the localized spin state. This state may then be measured using techniques developed for single spins.

The Hamiltonian in Eq. (1) can be mapped onto a variety of quantum field theories²⁷ via the Jordan-Wigner mapping. The spectrum resembles that of a semiconductor with a solitonlike defect state which is closely related to those in conducting polymers, inheriting many of the same properties such as spin-charge separation and topological stability.²⁵ Continuum field-theoretic descriptions²⁸ are also applicable to these dimerized spin systems, provided the defect extends over many spin lattice sites.

We now consider a specific parametrization $J_k = J_0 \exp[(-1)^k \alpha(k)]$ of the Hamiltonian in Eq. (1), where α is

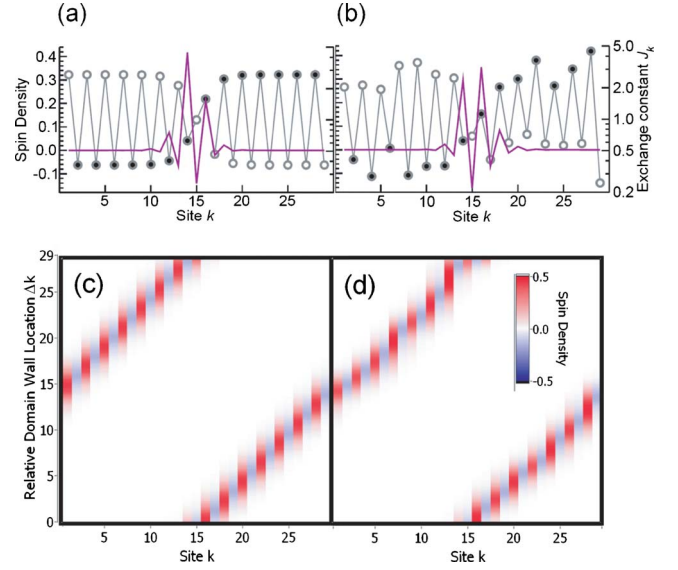


FIG. 2. (Color online) Generation of a flying spin qubit. (a) Exchange profile (circles) and spin density (line with no symbol) corresponding to the spin-up ground state for an $n_c=29$ spin ring containing a single solitonlike state. The filled circles represent even spin sites, and the empty circles represent odd spin sites. (b) Exchange profile and spin density for the spin-up ground state obtained when 50% multiplicative disorder is introduced into the exchange interaction strengths of the system in (a). (c) Adiabatic displacement of the qubit state shown in (a), achieved by shifting the domain wall center position by an amount Δk relative to its initial position $k_0=15$. The ground state is separated from the first excited state by a gap $\sim J$ for all domain wall locations. (d) Adiabatic displacement of the qubit state for the disordered case shown in (b).

a staggered order parameter describing dimerization in the chain. Spatially localized qubits are produced at the zero crossings of α and represent particlelike excitations of a designer quantum field. We illustrate the localization of these qubits by considering a closed chain with $n_c=29$ and $J_0=1$ [Fig. 2(a)]. A single domain wall is centered at k_0 with width w for $\alpha(k-k_0) = a_0 \sum_{r=-\infty}^{\infty} (-1)^r \tanh[(k-(k_0+rm_c)]/w$, where $a_0=1$, $k_0=15$, and $w=2$. The spin density of the spin-up ground state is determined by numerical Lanczos diagonalization and is superimposed on the exchange profile, showing that localization coincides with the zero crossing of α . This localization is retained when 50% multiplicative disorder is introduced into the exchange interaction strengths [Fig. 2(b)], illustrating the stability of the qubit with respect to local perturbations of the exchange profile.

By moving the domain wall, it is possible to transport logical spin qubits in a way that preserves the quantum information. Movement of the qubit state around the entire ring, achieved by letting $k_0 \rightarrow k_0 + \Delta k$ and varying Δk , is shown in Fig. 2(c). To visualize the qubit, its spin density is plotted as a function of lattice site and domain wall displacement Δk . Note that two revolutions are required to achieve full periodicity for an n_c -odd spin ring. Variations in the energy gap $E_1 - E_0$ between the ground state E_0 , which represents the qubit, and the first excited state E_1 are small [$\Delta(E_1 - E_0)/(E_1 - E_0)_{\min} \approx 0.23$].

For all domain wall positions shown in Fig. 2, the magnitude of the gap $E_1 - E_0$ remains $\sim J$. The presence of a finite

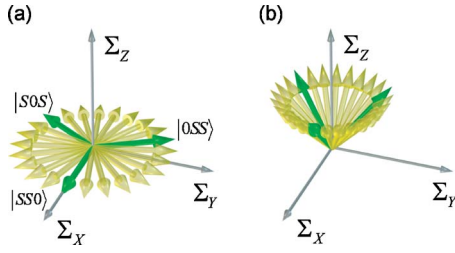


FIG. 3. (Color online) Analytical model. (a) Coherent evolution in the pseudo spin- $\frac{1}{2}$ space for an $n_c=3$ spin ring. Adiabatic evolution transports the spin state coherently between three nonorthogonal states shown as green arrows. (b) At high domain wall velocities, the Floquet states become distorted and eventually merge with eigenstates of Σ_Z .

energy gap serves to protect the quantum information encoded in the ground state from decoherence due to noise.^{29,30} This protective effect is evident from an analysis of the system in the case of static disorder: Figure 2(d) shows that as the domain wall center for the disordered system is displaced, the spatial localization of the qubit is preserved. Furthermore, because the exchange Hamiltonian in Eq. (1) conserves S^2 and S_Z , these eigenvalues are unchanged by the introduction of noise into the exchange interaction strengths. Note that this reasoning is applicable in general, so that the finite gap $E_1 - E_0$ and the conservation of S^2 and S_Z will preserve the quantum information whether the noise is static or time dependent.

III. ANALYTICAL MODEL

General features of flying spin qubits emerge from an analysis of the simplest nontrivial case $n_c=3$, for which exact solutions exist. The most general $n_c=3$ Hamiltonian in Eq. (1) can be reparametrized as

$$H_3 = \sum_{k=1}^3 [\tilde{J}_0 + \tilde{J}_1 \cos(2\pi(k-1)/3 - \varphi)] \mathbf{S}_k \cdot \mathbf{S}_{k+1}, \quad (2)$$

where \tilde{J}_0 and \tilde{J}_1 are constants, and φ represents the phase of the domain wall around the ring. The $(S, S_Z) = (1/2, 1/2)$ subspace is two dimensional, spanned by the states $|\pm\rangle = |001\rangle + e^{\pm 2\pi i/3}|010\rangle + e^{\pm 4\pi i/3}|100\rangle$. (Here and in the following analysis, the states are defined up to an overall normalization factor.) Using this basis, we can re-express $H_3(\varphi) = \frac{\Delta}{2}(\Sigma_X \cos \varphi + \Sigma_Y \sin \varphi) - \frac{3\tilde{J}_0}{4}\mathbf{1}$, where the energy gap between the ground and first excited states is $\Delta = 3\tilde{J}_1/2$ and $\Sigma_{X\pm iY} \equiv \frac{4}{3} \sum_{k=1}^3 e^{\pm 2\pi i(k-1)/3} \mathbf{S}_k \cdot \mathbf{S}_{k+1}$. Together with $\Sigma_Z = -\frac{1}{2}[\Sigma_X, \Sigma_Y]$, the operators $\{\Sigma_X, \Sigma_Y, \Sigma_Z\}$ satisfy $[\Sigma_a, \Sigma_b] = 2i\epsilon_{abc}\Sigma_c$, and the states $\{|\pm\rangle\}$ can be regarded as a pseudospin doublet [Fig. 3(a)]. This two-dimensional space is identical to the three-spin qubit proposed by DiVincenzo *et al.* in Ref. 10, but it does not represent the qubit; rather, it represents an orbital degree of freedom for the spin-up state. An isomorphic two-dimensional subspace exists for the spin-down state. Spatially uniform exchange (parametrized by \tilde{J}_0)

does not couple to these states, and the ground state energy of $H_3(\varphi)$ is independent of φ . We can interpret $\{|\pm\rangle\}$ as right- and left-traveling spin-current Bloch states, eigenstates of the discrete translation operator D_2 (defined by $D_2 \mathbf{S}_k \equiv \mathbf{S}_{k+2} D_2$) over two lattice sites. The ground state of $H_3(\varphi)$ is given by $|\varphi\rangle \equiv |+\rangle - e^{i\varphi}|-\rangle$. The case $\varphi=0$ yields explicitly $|\varphi=0\rangle = |010\rangle - |100\rangle \equiv |SS0\rangle$, which corresponds to spins 1 and 2 being in a singlet state, and spin 3 being in the “0” state. Adiabatic evolution of φ coherently moves the spin qubit around the ring, such that $|\varphi=2\pi/3\rangle = |001\rangle - |010\rangle \equiv |OSS\rangle$ and $|\varphi=4\pi/3\rangle = |001\rangle - |100\rangle \equiv |SOS\rangle$. Note that these three states are not mutually orthogonal—they cannot be, since the space in which they evolve is two dimensional.

By letting $\varphi = \omega t$, the domain wall can be moved at a constant speed [Fig. 3(b)]. Because the Hamiltonian is now explicitly time dependent, there are no longer stationary states; however, one may employ Bloch-Floquet theory³¹ to understand the steady-state dynamics. The time evolution is governed by a unitary operator U_t that satisfies the Schrödinger equation $i\partial_t U_t = H(t)U_t$, subject to the initial condition $U_0 = \mathbf{1}$. Floquet states are defined here to be the eigenstates of the combined time and space translation operators, $F = D_2 U_{4\pi/n_c\omega}$. Full translation around a closed spin chain by two revolutions (governed by the operator F^{n_c} or, equivalently, $U_{4\pi/\omega}$) yields the same Floquet states as for F .

For the three-spin ring, we obtain the remarkable exact result for the Floquet state associated with the ground state:

$$|X+; \pm \omega\rangle = |SS0\rangle + \left[\frac{\omega}{\Delta} \pm \sqrt{1 + \left(\frac{\omega}{\Delta}\right)^2} \mp 1 \right] |\pm\rangle, \quad \omega > 0. \quad (3)$$

This state can be interpreted as a “snapshot” of the steady-state quantum dynamics at intervals in time $t = 0, 2\pi/\omega, 4\pi/\omega, \dots$, and is valid for all ω . The adiabatic regime can be defined to be the range $|\omega| < \Delta$, in accordance with the energy-time uncertainty principle.

The exact results obtained for the three-spin ring extrapolate well to larger systems. To demonstrate, we consider an $n_c=9$ spin ring with a single domain wall given by $J_k = J_0 + (-1)^k \alpha'(k-k_0)$, where $J_0=1$ and $\alpha'(k-k_0) = a_0 \sin(\pi(k-k_0)/n_c - \omega t)$. With $k_0 \rightarrow k_0 + \frac{n_c}{\pi} \omega t$, the staggered order parameter corresponds to $\alpha(k-k_0) = a_0 \sum_{r=-\infty}^{\infty} (-1)^r \tanh[\pi(k - (k_0 + r n_c))/w]$ in the limit $w \rightarrow n_c$. Choosing $a_0=0.1$ and $k_0 = n_c/2$, we obtain the Floquet states of the operator $D_2 U_{2\pi/n_c\omega}$ for the $n_c=9$ spin ring. The ground state $|\varphi_s^0\rangle$ is the analog of the state $|SS0\rangle$ in Eq. (3), where each spin in Eq. (3) has been replaced by a three-spin cluster qubit.¹³ The state $|\varphi_s^0\rangle$ is determined by numerical diagonalization of the initial Hamiltonian. We also find that the Floquet state $|\varphi_s(\omega)\rangle$ associated with the ground state for $\omega < \Delta E$ is well approximated (to within 1%) by the following expression:

$$|\varphi_s^{\text{th}}(\omega)\rangle = |\varphi_s^0\rangle + \frac{\omega}{\Delta E} |+\rangle, \quad (4)$$

where $|+\rangle = \frac{1}{\sqrt{2}}(|u_1^0\rangle + i|u_2^0\rangle)$ is an eigenstate of D_2 for the $n_c=9$ spin ring, and $|u_1^0\rangle$ and $|u_2^0\rangle$ are the ground states of this ring for the case $J_k=1$. The energy gap ΔE between the

ground state and the first excited state is finite and is independent of the position of the domain wall. We note here that, for a given maximum value of the angular speed ω , if the qubit speed is increased instantaneously to ω , the error in the overlap $|\langle \varphi_s(\omega) | \varphi_s^0 \rangle|^2$ increases as $\sim \omega^2$. From Eq. (3), it can be seen that this $\sim \omega^2$ dependence of the error also exists for the three-spin ring. Nevertheless, if the speed of the qubit is allowed to increase adiabatically to its maximum value ω in small steps of $\delta\omega \equiv \omega/N$, where N is the number of steps, the error for each such step is proportional to $\delta\omega^2 = (\omega/N)^2$. Thus, provided $\omega < \Delta E$, as N is made very large, $|\varphi_s(\omega)\rangle \rightarrow |\varphi_s^0\rangle$ and the fidelity of qubit transfer may be made arbitrarily close to unity.

IV. EINSTEIN-PODOLSKY-ROSEN PAIR GENERATION

We now discuss a method of generating EPR pairs from a fully dimerized spin chain. Numerical investigations are performed for a closed chain with $n_c=30$ spins, using Lanczos diagonalization to determine the spin density and energies. The system is assumed to be initialized in the spin-singlet ground state ($S=0$). Two domain walls, denoted A and B , are created and moved in opposite directions [Fig. 4(a)]. The exchange profile describing this system is given by $J_k = 0.55 - 0.45(-1)^k[1 + \alpha(k - k_A) - \alpha(k - k_B)]$, where $k_A = (n_c + s)/2$, $k_B = (n_c - s)/2$, and s is the separation between the two domain walls. Note that the exact quantitative form of the exchange profile is not crucial to this method of producing EPR pairs, provided the general characteristics which produce the domain walls are retained in the profile.

Because the exchange interaction conserves S , the two qubits associated with the domain walls must exist in a spin singlet or EPR pair: $|\psi_0\rangle = \frac{1}{\sqrt{2}}(|\uparrow\rangle_A |\downarrow\rangle_B - |\downarrow\rangle_A |\uparrow\rangle_B)$. In order to visualize this state, one can hybridize it with the first excited (triplet) state $|\psi_1\rangle = \frac{1}{\sqrt{2}}(|\uparrow\rangle_A |\downarrow\rangle_B + |\downarrow\rangle_A |\uparrow\rangle_B)$ and compute the spin density for $\frac{1}{2}(|\psi_0\rangle - |\psi_1\rangle) = |\downarrow\rangle_A |\uparrow\rangle_B$ [Fig. 4(b)]. The energies of the three lowest states behave as expected: there is an exchange splitting $\Delta E = E_1 - E_0$ for the two spin qubits which decreases exponentially as the domain walls are moved apart [Fig. 4(c)]. The next excited state (energy E_2) is given approximately by the one-magnon gap energy,³² which is largely unaffected by the domain wall states (i.e., $E_2 - E_0$ is approximately constant). Within a larger system, it would be possible to “radiate” multiple EPR pairs. Because they are entangled states, EPR pairs constitute an important physical resource for applications such as quantum teleportation.²⁴

V. PHYSICAL REALIZATION

The proposed mechanism for flying spin qubits must be capable of implementation in order to be relevant for quantum computing architectures. Here, we describe a specific realization using a one-dimensional array of elliptically shaped quantum dots, each containing one spin- $\frac{1}{2}$ electron (Fig. 5). Application of an electric field transverse to the array axis modulates the exchange interaction strength between each pair of nearest-neighbor quantum dots [Fig. 5(a)]. Each zero crossing of the electric field corresponds to

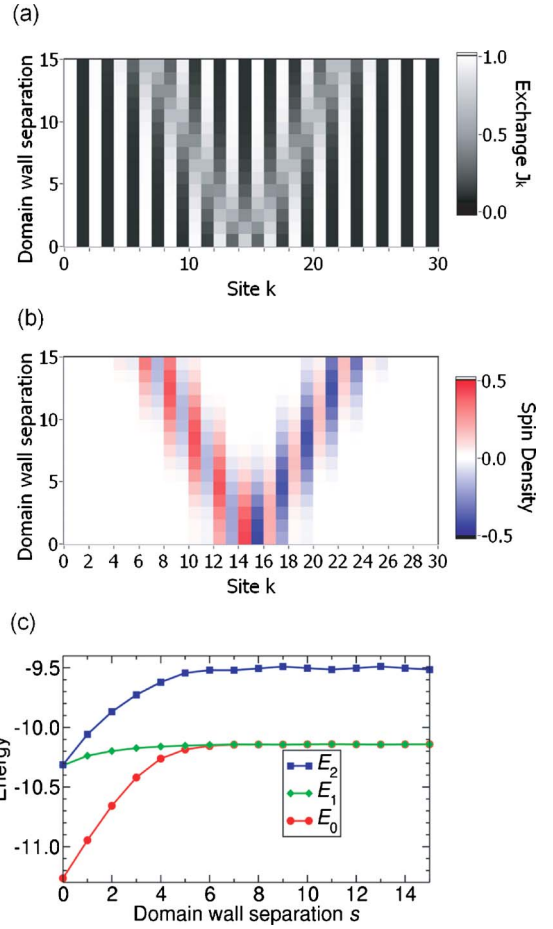


FIG. 4. (Color online) (a) Exchange profile for an $n_c=30$ spin chain that is initially dimerized uniformly ($J_{k=\text{odd}}=1.0$, $J_{k=\text{even}}=0.1$). A domain wall pair is produced, and the walls move outward, creating an entangled pair of solitonlike states. (b) Spin density for a linear combination of the (spin-up) ground and first excited states, showing spatial separation of the qubit states as expected. (c) Lowest three energies (in units of J) as a function of the domain wall separation s , showing the expected exchange splitting between E_0 and E_1 , and a relatively constant spin-wave gap between E_0 and E_2 .

a single (flying) spin qubit [Fig. 5(b)]. The “pseudodigital” nature³³ of $J(E)$, dependent on the detailed shape of the quantum dots, produces qubits that become more localized with increasing electric field amplitude. The electric field required to transport flying spin qubits may be implemented in a variety of ways, e.g., using a suitably designed coplanar waveguide.

The rate of qubit transfer R for such a device can be estimated in terms of the nominal exchange strength J between nearest-neighbor dots and the domain wall width w . The energy gap for the qubit states scales as $\Delta \sim J/w$, similar to that for spin cluster qubits.¹³ The qubit can travel w sites in a time \hbar/Δ without violating the energy-time uncertainty principle. Taking $D \approx 100$ sites for the spacing between domain walls, and using parameters relevant to Ge/Si quantum dots³⁴ separated by $d=35$ nm and coupled by direct

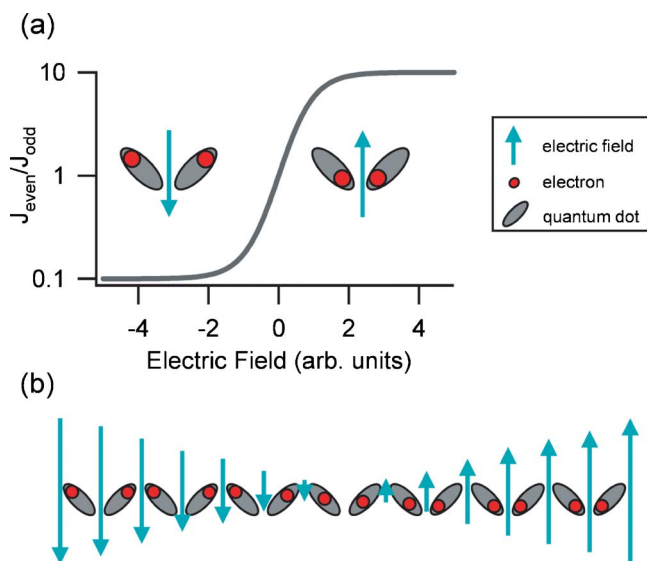


FIG. 5. (Color online) Experimental realization for flying spin qubits. (a) Dimerized exchange $J(E)$ produced by elliptically shaped quantum dots in a transverse electric field. The field profile maps directly onto the staggered order parameter α . (b) Zero crossings of the electric field correspond to single qubit states.

exchange $J_0 \sim 500 \mu\text{eV}$,³⁵ one obtains $R = J_0/\hbar D$ qubit $\approx 7.6 \times 10^9$ qubit/s. Limitations on the switching speed for the electric field may reduce the qubit transfer rate from this maximum value; however, the mechanism of electric field

propagation itself does not limit the rate. Sources of decoherence relevant to electron spins in quantum dots, such as fluctuating fields and coupling to nuclear spins, also apply to the systems considered here.^{1,13}

Flying spin qubits should prove useful at all architectural levels, such as transporting “fresh qubits” for quantum error correction, carrying qubits to readout locations, implementing quantum gating between remote qubits, and other tasks.

VI. CONCLUSION

In summary, we have demonstrated a mechanism by which flying spin qubits can be produced and moved controllably entirely within the solid state. Rapid, high-fidelity transport of spin qubits is achieved by designing a quantum field with solitonlike domain walls that support localized spin states. The qubits created in this manner are topologically stable with respect to local perturbations of the exchange profile. By creating pairs of domain walls from a uniformly dimerized state, EPR pairs may be efficiently generated. Finally, we have proposed a scheme for implementing flying spin qubits in an array of elliptically shaped quantum dots.

ACKNOWLEDGMENTS

We thank Yaakov Weinstein for helpful comments. Computations were performed at the ASC DoD Major Shared Resource Center.

*vas9@pitt.edu

†jlevy@pitt.edu

‡hellberg@nrl.navy.mil

¹D. Loss and D. P. DiVincenzo, Phys. Rev. A **57**, 120 (1998).

²B. E. Kane, Nature (London) **393**, 133 (1998).

³V. Privman, I. D. Vagner, and G. Kventsel, Phys. Lett. A **239**, 141 (1998).

⁴A. Imamoglu, D. D. Awschalom, G. Burkard, D. P. DiVincenzo, D. Loss, M. Sherwin, and A. Small, Phys. Rev. Lett. **83**, 4204 (1999).

⁵R. Vrijen, E. Yablonovitch, K. Wang, H. W. Jiang, A. Balandin, V. Roychowdhury, T. Mor, and D. DiVincenzo, Phys. Rev. A **62**, 012306 (2000).

⁶J. Levy, Phys. Rev. A **64**, 052306 (2001).

⁷T. D. Ladd, J. R. Goldman, F. Yamaguchi, Y. Yamamoto, E. Abe, and K. M. Itoh, Phys. Rev. Lett. **89**, 017901 (2002).

⁸P. Zanardi and M. Rasetti, Phys. Rev. Lett. **79**, 3306 (1997).

⁹D. A. Lidar, I. L. Chuang, and K. B. Whaley, Phys. Rev. Lett. **81**, 2594 (1998).

¹⁰D. P. DiVincenzo, D. Bacon, J. Kempe, G. Burkard, and K. B. Whaley, Nature (London) **408**, 339 (2000).

¹¹J. Levy, Phys. Rev. Lett. **89**, 147902 (2002).

¹²P. W. Shor, Phys. Rev. A **52**, R2493 (1995).

¹³F. Meier, J. Levy, and D. Loss, Phys. Rev. Lett. **90**, 047901 (2003).

¹⁴P. Jordan and E. P. Wigner, Z. Phys. **47**, 631 (1928).

¹⁵E. Fradkin, Phys. Rev. Lett. **63**, 322 (1989).

¹⁶C. D. Batista and G. Ortiz, Phys. Rev. Lett. **86**, 1082 (2001).

¹⁷D. P. DiVincenzo, Fortschr. Phys. **48**, 771 (2000).

¹⁸S. Bose, Phys. Rev. Lett. **91**, 207901 (2003).

¹⁹M. Christandl, N. Datta, A. Ekert, and A. J. Landahl, Phys. Rev. Lett. **92**, 187902 (2004).

²⁰A. Wojcik, T. Luczak, P. Kurzynski, A. Grudka, T. Gdala, and M. Bednarska, Phys. Rev. A **72**, 034303 (2005).

²¹G. De Chiara, D. Rossini, S. Montangero, and R. Fazio, Phys. Rev. A **72**, 012323 (2005).

²²A. M. Steane, Quantum Inf. Comput. **2**, 297 (2002).

²³T. Szkopek, P. O. Boykin, H. Fan, V. P. Roychowdhury, E. Yablonovitch, G. Simms, M. Gyure, and B. Fong, IEEE Trans. Nanotechnol. **5**, 42 (2006).

²⁴C. H. Bennett, G. Brassard, C. Crepeau, R. Jozsa, A. Peres, and W. K. Wootters, Phys. Rev. Lett. **70**, 1895 (1993).

²⁵A. J. Heeger, S. Kivelson, J. R. Schrieffer, and W.-P. Su, Rev. Mod. Phys. **60**, 781 (1988).

²⁶J. Cullum and R. A. Willoughby, *Lanczos Algorithms for Large Symmetric Eigenvalue Computations* (Birkhauser, Boston, 1985).

²⁷A. Auerbach, *Interacting Electrons and Quantum Magnetism* (Springer-Verlag, New York, 1994).

²⁸T. Nakano and H. Fukuyama, J. Phys. Soc. Jpn. **49**, 1679 (1980).

²⁹D. Bacon, K. R. Brown, and K. B. Whaley, Phys. Rev. Lett. **87**, 247902 (2001).

- ³⁰Y. S. Weinstein and C. S. Hellberg, Phys. Rev. Lett. **98**, 110501 (2007).
- ³¹J. H. Shirley, Phys. Rev. **138**, B979 (1965).
- ³²T. Barnes, J. Riera, and D. A. Tennant, Phys. Rev. B **59**, 11384 (1999).
- ³³M. Friesen, R. Joynt, and M. A. Eriksson, Appl. Phys. Lett. **81**, 4619 (2002).
- ³⁴O. Guise, J. Ahner, J. J. T. Yates, V. Vaithyanathan, D. G. Schlom, and J. Levy, Appl. Phys. Lett. **87**, 171902 (2005).
- ³⁵C. Pryor and M. E. Flatté (unpublished).